

Isomeric Ionic Lithium Isonicotinate Three-Dimensional Networks and Single-Crystal-to-Single-Crystal Rearrangements Generating Microporous Materials

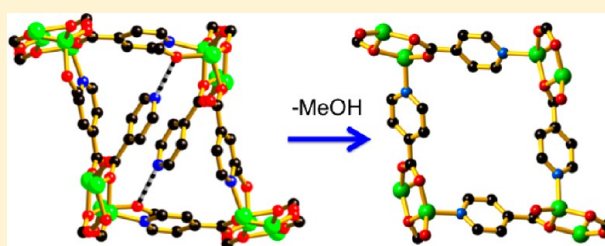
Brendan F. Abrahams,^{*,†} A. David Dharma,[†] Martin J. Grannas,[†] Timothy A. Hudson,[†] Helen E. Maynard-Casely,^{‡,§} Graham R. Oliver,[†] Richard Robson,^{*,†} and Keith F. White[†]

[†]School of Chemistry, University of Melbourne, Grattan Street, Parkville, Victoria 3010 Australia

[‡]Australian Synchrotron, 800 Blackburn Road, Clayton, Victoria 3168, Australia

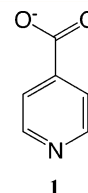
Supporting Information

ABSTRACT: Reaction between LiOH and isonicotinic acid (inicH) in the appropriate solvent or mixture of solvents affords a family of variously solvated forms of a simple ionic lithium salt, *viz.*, Li⁺inic⁻·S (where S = 0.5 morpholine, 0.5 dioxane, 0.25 *n*-hexanol, 0.5 *N*-methylpyrrolidinone, 0.5 *N,N*-dimethylformamide, 0.5 *n*-propanol, 0.5 cyclohexanol, 0.5 pyridine, 0.5 *t*-butanol, 0.5 ethanol, and 0.5 methanol). Three-dimensional Li⁺inic⁻ frameworks containing solvent-filled channels are present in all of these except for the MeOH and EtOH solvates. The nondirectional character of the electrostatic interactions between the Li⁺ and inic⁻ ions bestows an element of “plasticity” upon the framework, manifested in the observation of no less than five different framework structures within the family. Unusual single-crystal-to-single-crystal transformations accompany desolvation of Li⁺inic⁻·S in which the Li⁺inic⁻ framework undergoes a major rearrangement (from a structure containing “8484 chains” to one with “6666 chains”). The “before and after” structures are strongly suggestive of the mechanism and the driving force for these solid state framework rearrangements: processes which further demonstrate the “plasticity” of the ionic Li(inic) framework. A solid-state mechanism for these desolvation processes that accounts very satisfactorily for the formation of the channels and for the diverse geometrical/topological aspects of the transformation is proposed. The reverse process allows the regeneration of the solvated 8484 form. When the 6666 Li⁺inic⁻ form is immersed in carbon disulfide, a single-crystal-to-single-crystal transformation occurs to generate Li⁺inic⁻·0.25CS₂. The hydrate, Li⁺inic⁻·2H₂O which consists of discrete Li(inic)·H₂O chains obtained by recrystallizing the salt from water, can also be obtained by hydration of the 6666 form. A dense 3D network with the formula, Li(inic) can be obtained in a reversible process by the removal of the water from the hydrated form and also by crystallization from a *t*-amyl alcohol solution.



INTRODUCTION

Zeolitic aluminosilicates, because of their channel-containing structures, have long been used commercially in sorption, separation, and catalysis.¹ A number of other classes of microporous materials has more recently been introduced and studied with similar possible applications in mind — materials such as carbon nanotubes,² activated carbon materials,³ and coordination polymers, also referred to as MOFs.⁴ Following the report by Kitagawa and co-workers of gas storage in coordination polymers in 1997⁵ there was an upsurge of activity in this area that continues to this day.⁶ One important potential application of porous coordination polymers relates to the storage of gaseous fuels such as hydrogen and methane for mobile uses. Desirable features of such materials include not only high gas sorption capacities but also isosteric heat of sorption values that will allow controllable release of gases under conditions of pressures and temperatures that are easily achieved in mobile systems. Porous materials possessing large intraframework voids are able to exhibit high hydrogen storage capacities, but unfortunately they commonly

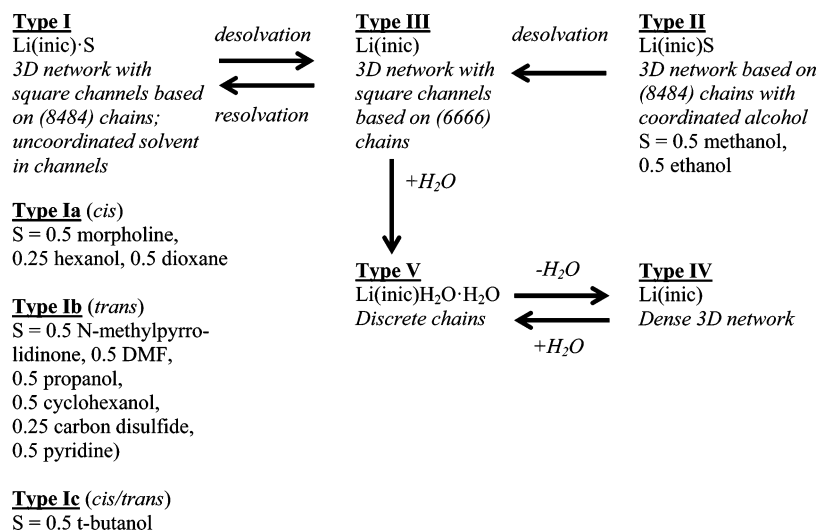


display isosteric heat of sorption values in the range -5 to -7 kJ mol^{-1} .⁷ As a consequence these materials host only small quantities of hydrogen under mild pressures and ambient temperature. In order for significant quantities of hydrogen to be retained in porous coordination polymers under the types of conditions that could make onboard hydrogen storage economically viable, isosteric heat of sorption values in the range -15 to -25 kJ mol^{-1} are required.⁸ One approach to obtaining coordination polymers with higher (more negative) heat of sorption values is to employ materials with smaller

Received: December 27, 2013

Published: May 8, 2014

Scheme 1. Summary of Structural Types for Li(inic) Frameworks



pores. Materials with smaller pores tend to have higher densities, and thus, the maximum amount of hydrogen that may be stored per unit mass of framework is generally lower when the pores are smaller.⁹ If small pore networks were to be used in order to take advantage of superior heat of sorption values, it would seem important for the mass of the host network to be as low as possible; thus lightweight components including metals such as lithium, magnesium, and aluminum are obvious choices for exploration.¹⁰ Networks derived from these metals (as well as others from the *s* block elements) have been reviewed recently by Parise and Banerjee,¹¹ Zaworotko et al.,¹² Eddaoudi and co-workers,¹³ as well as Feng et al.¹⁴ have also reported recent examples of lithium based open-type networks.

The energy of an electrostatically bound system is dependent only on the separation between charges and is independent of direction. This nondirectional character of ionic bonding seemed to us a very desirable property to be incorporated into infinite networks (if indeed such ionic networks could be constructed) because it might bestow a degree of “plasticity” on the framework allowing it to flex and thereby to maximize favorable interactions with various intercalated guests. On the basis of this sort of consideration, we have undertaken a synthetic and structural exploration of a variety of simple salts in which the Li⁺ cation is combined with a range of anions possessing some degree of internal rigidity, in the hope of discovering new classes of essentially ionic but microporous materials.

In a recent preliminary note the synthesis and structural study of three differently solvated forms of a simple ionic lithium salt, namely Li⁺inic⁻·S (where inic⁻ = the isonicotinate anion, **1**, and S = 0.5 *N,N*-dimethylformamide or 0.5 *N*-methylpyrrolidinone or 0.5 morpholine), were reported; removal of the guests afforded materials showing reversible sorption of various gases.¹⁵ Gas sorption studies of the desolvated Li⁺inic⁻ network indicated the uptake of marked quantities of hydrogen [86 mL (STP) g⁻¹ at 640 kPa and 77 K], carbon dioxide [83 mL (STP) g⁻¹ at 2160 kPa and 258 K], and methane [62 mL (STP) g⁻¹ at 3040 kPa and 258 K]. Of particular note was the determination of relatively high isosteric heat of sorption values for hydrogen (−9.9 kJ mol⁻¹) and carbon dioxide (−34.5 kJ mol⁻¹) which we attributed to the small pore size of the network.¹⁵ In the present Article we

report an extended range of compounds in the Li(inic)·S family, whose structures reveal a form of framework isomerism that had previously escaped notice. We are now aware of no less than six different topologies and structures for the 3D Li(inic) framework which are described below in addition to a hydrated form that has a chain structure. Scheme 1 provides a summary of the structural types found for the Li(inic) frameworks. Also reported are examples of solid-state transformation including unusual single-crystal-to-single-crystal transformations accompanying desolvation and resolution during which the ionic Li(inic) framework undergoes profound rearrangements. The “before and after” structures provide insight into the mechanism and the driving force for these solid-state framework rearrangements.

EXPERIMENTAL SECTION

General Procedures. Commercially available reagents employed in the synthesis of the compounds reported were used without further purification. Microanalyses were performed by either the Microanalytical Unit in the Research School of Chemistry at the Australian National University or the Campbell Microanalytical Laboratory at the University of Otago, New Zealand.

Li(inic)·S (Type I). S = 0.5 morpholine, 0.5 dioxane, 0.25 *n*-hexanol, 0.5 *N*-methylpyrrolidinone, 0.5 *N,N*-dimethylformamide, 0.5 *n*-propanol, 0.5 cyclohexanol, 0.5 pyridine, 0.5 *t*-butanol.

The following procedure for the synthesis of the type **Ia** Li(inic)·0.5dioxane is a typical example for all of the Li(inic)·S (type **I**) compounds. Specific details for the synthesis of the remaining Li(inic)·S (type **I**) solvates are presented in the Supporting Information. Isonicotinic acid (106 mg, 0.86 mmol) and LiOH·H₂O (35 mg, 0.83 mmol) were dissolved in boiling methanol (5 mL). Dioxane (5 mL) was then added to the boiling solution with further heating. When the vapor temperature approached the boiling point of dioxane, colorless crystals separated from the solution. Upon cooling, the crystals were collected, washed with dioxane, and dried in air. Yield: 59%. Anal. Found: C, 46.9; H, 4.7; N, 8.1. Calcd for Li(inic)·0.2dioxane·1.5H₂O: C, 47.0; H, 5.0; N, 8.1%.

Li(inic)·S (Type II). S = 0.5 MeOH and 0.5 EtOH.

The following procedure for the synthesis of the type **II** Li(inic)·0.5MeOH is similar to that employed for the ethanol solvate. Specific details for the synthesis of the second (type **II**) compound, Li(inic)·EtOH, are presented in the Supporting Information.

Isonicotinic acid (200 mg, 1.6 mmol) and LiOH·H₂O (68.3 mg, 1.6 mmol) were dissolved in boiling MeOH (20 mL). Acetonitrile (25 mL) was added to the boiling solution. The temperature of the

Table 1. Crystal Data and Refinement Details

	Li(inc)-0.5 morpholine ^a	Li(inc)-0.5 dioxane	Li(inc)-0.25 <i>n</i> -hexanol	Li(inc)-0.5 <i>N</i> -methyl-pyrrolidinone ^a	Li(inc)-0.5 <i>N,N</i> -dimethyl-formamide ^a	Li(inc)-0.5 <i>n</i> -propanol	Li(inc)-0.5 cyclohexanol	Li(inc)-0.5 pyridine
formula	C ₁₆ H ₁₇ Li ₂ N ₃ O ₅	C ₁₆ H ₁₆ Li ₂ N ₂ O ₆	C ₃₀ H ₃₀ Li ₄ N ₄ O ₉	C ₁₇ H ₁₇ Li ₂ N ₃ O ₅	C ₁₅ H ₁₅ Li ₂ N ₃ O ₅	C ₃₀ H ₃₂ Li ₄ N ₄ O ₁₀	C ₁₈ H ₂₀ Li ₂ N ₂ O ₅	C ₁₇ H ₁₃ Li ₂ N ₃ O ₄
<i>M_r</i>	345.21	346.19	618.34	357.22	331.18	636.36	358.24	337.18
cryst syst	triclinic	triclinic	monoclinic	monoclinic	monoclinic	monoclinic	monoclinic	monoclinic
space group	<i>P</i> $\bar{1}$	<i>P</i> $\bar{1}$	<i>P</i> 2 ₁ / <i>c</i>	<i>P</i> 2 ₁	<i>P</i> 2 ₁ / <i>n</i>	<i>P</i> 2 ₁	<i>P</i> 2 ₁ / <i>n</i>	<i>P</i> 2 ₁ / <i>n</i>
<i>a</i> /Å	5.3968(3)	5.3992(2)	10.8681(2)	5.47330(10)	5.40280(10)	10.80930(10)	5.3881(8)	5.4241(4)
<i>b</i> /Å	11.4886(9)	11.1408(6)	9.8358(3)	13.4580(2)	13.9175(2)	14.3476(2)	14.118(2)	13.8293(9)
<i>c</i> /Å	13.4233(9)	13.6811(8)	14.6059(3)	11.7304(2)	11.2862(3)	10.82430(10)	11.410(2)	11.1181(9)
α /deg	90.670(6)	90.885(5)	90	90	90	90	90	90
β /deg	94.900(5)	94.250(4)	94.096(2)	101.166(2)	102.875(2)	103.5590(10)	101.187(15)	102.790(9)
γ /deg	91.238(6)	91.825(4)	90	90	90	90	90	90
<i>V</i> /Å ³	828.96(10)	820.13(7)	1557.33(6)	847.70(2)	827.31(3)	1631.93(3)	851.4(2)	813.29(10)
<i>Z</i>	2	2	2	2	2	2	2	2
<i>w</i> R2 (all data)	0.2267	0.2235	0.1782	0.1032	0.2151	0.0875	0.2736	0.1825
<i>R</i> 1 (<i>I</i> > 2 σ (<i>I</i>))	0.0838	0.0752	0.0568	0.0393	0.0649	0.0309	0.0902	0.0601
GOF	1.158	1.092	1.116	1.082	1.123	0.765	0.967	1.063
	Li(inc)-0.5 <i>t</i> -butanol	Li(inc)-0.5methanol	Li(inc)-0.5ethanol	Li(inc) type III	Li(inc)-0.25carbon disulfide	Li(inc) type IV	Li(inc)-2H ₂ O	
formula	C ₃₂ H ₃₆ Li ₄ N ₄ O ₁₀	C ₁₃ H ₁₂ Li ₂ N ₂ O ₅	C ₁₄ H ₁₄ Li ₂ N ₂ O ₅	C ₆ H ₄ LiNO ₂	C ₂₅ H ₁₆ Li ₄ N ₄ O ₈ S ₂	C ₁₂ H ₈ Li ₂ N ₂ O ₄	C ₆ H ₈ LiNO ₄	
<i>M_r</i>	664.41	290.13	304.15	129.04	592.30	258.08	165.07	
cryst syst	triclinic	monoclinic	monoclinic	orthorhombic	monoclinic	monoclinic	monoclinic	
space group	<i>P</i> $\bar{1}$	<i>P</i> 2 ₁ / <i>n</i>	<i>P</i> 2 ₁ / <i>n</i>	<i>P</i> na2 ₁	<i>P</i> 2 ₁ / <i>c</i>	<i>P</i> 2 ₁ / <i>n</i>	<i>C</i> c	
<i>a</i> /Å	5.4013(8)	10.2402(5)	10.41750(10)	10.680(2)	5.2038(14)	5.21200(10)	7.1563(8)	
<i>b</i> /Å	17.644(2)	9.5023(4)	9.59220(10)	13.732(2)	14.516(7)	18.8836(6)	18.8826(12)	
<i>c</i> /Å	17.825(3)	15.2912(6)	15.2877(2)	4.9114 (10)	10.295(5)	11.8624(3)	6.2227(6)	
α /deg	89.391(12)	90	90	90	90	90	90	
β /deg	85.708(13)	98.328(4)	97.4790(10)	90	96.14(4)	101.984(3)	115.463(13)	
γ /deg	86.268(11)	90	90	90	90	90	90	
<i>V</i> /Å ³	1690.3(4)	1472.23(11)	1514.65(3)	720.3(3)	773.6(6)	1142.07(5)	759.19(12)	
<i>Z</i>	2	4	4	4	1	4	4	
<i>w</i> R2 (all data)	0.0922	0.2727	0.0982	0.1748	0.6205	0.0931	0.1057	
<i>R</i> 1 (<i>I</i> > 2 σ (<i>I</i>))	0.0438	0.0952	0.0379	0.0628	0.2788	0.0334	0.0343	
GOF	0.726	1.274	1.051	1.089	1.743	1.063	1.126	

^aReported in preliminary communication.¹⁵

solution was held at 50 °C in an open flask. The gradual evaporation of the reaction mixture to approximately half the initial volume caused the separation of colorless crystals, which were collected and dried briefly under a flow of air. Yield: 217 mg (83%). Anal. Found: C, 53.9; H, 3.5; N, 10.3. Calcd for Li(inc)-0.1MeOH-0.25H₂O: C, 53.5; H, 3.6; N, 10.2%.

Li(inc) (Type III). A sample of Li(inc)-0.5 MeOH crystals were heated at 90 °C under a stream of N₂ for 4 h resulting in single crystals of Li(inc) (type III). Anal. Found: C, 55.4; H, 3.1; N, 10.7. Calcd for Li(inc): C, 55.8; H, 3.1; N, 10.9%.

Similar procedures for the generation of Li(inc) (type III) crystals were also employed when using the starting material Li(inc)-S (S = 0.5 morpholine, 0.5 DMF, 0.5 *n*-propanol, 0.5 *t*-butanol, 0.25 *n*-hexanol, 0.5 pyridine, 0.5 dioxane).

Li(inc) (Type IV). Isonicotinic acid (102 mg, 0.83 mmol) and LiOH·H₂O (38 mg, 0.90 mmol) were dissolved in boiling methanol (5 mL). *t*-Amyl alcohol (5 mL) was added to the boiling solution, which was further heated, and the vapor temperature was monitored. As the vapor temperature of the reaction mixture approached the boiling point of *t*-amyl alcohol, clear needle-shaped crystals separated from the hot solution. Anal. Found: C, 53.9; H, 3.4; N, 10.4. Calcd for Li(inc): C, 53.9; H, 3.4; N, 10.5%.

Li(inc)-2H₂O (Type V). Isonicotinic acid (100 mg, 0.81 mmol) and LiOH·H₂O (33 mg, 0.81 mmol) were dissolved in water (5 mL) and allowed to stand in an open flask. The evaporation of the water to almost dryness allowed colorless plate crystals to separate from the

solution. Yield: 60%. Anal. Found: C, 43.9; H, 4.9; N, 8.5. Calcd for Li(inc)-2H₂O: C, 43.7; H, 4.9; N, 8.5%.

Crystal Transformations. Li(inc) (Type III) to Li(inc) (Type I). Li(inc) (type III) crystals were immersed in CS₂ for 5 h. Crystals of Li(inc)-0.25CS₂ were then transferred directly from the solutions to a protective oil. A crystal was selected and placed on a single-crystal diffractometer in a stream of nitrogen at 130 K.

Li(inc) (type III) crystals were immersed in DMF for 5 h. A DMF slurry of the microcrystalline material was transferred to a Lindeman glass capillary tube which was sealed. Powder diffraction measurements were performed on the material in the Lindeman tube.

Li(inc) (Type IV) to Li(inc)-2H₂O (Type V). A sample of Li(inc) (type V) crystals were separated from the *t*-amyl mother liquor and subsequently exposed to the atmosphere over a period of a day. Powder diffraction confirmed the crystals had undergone a transformation to the Li(inc)-2H₂O (type V) structure (see Supporting Information).

Li(inc)-2H₂O (Type V) to Li(inc) (Type IV). A crystalline sample of Li(inc)-2H₂O was heated at 150 °C for a period of 3 h. Powder diffraction confirmed the crystals had undergone a transformation to the dense Li(inc) (type V) structure.

Crystallography. Single-crystal X-ray data were measured using Oxford Diffraction Supernova or Excalibur diffractometers using Cu K α radiation. Prior to the crystal being mounted on a goniometer the crystals were immersed in a protective oil to protect the crystals from loss of solvent. All data were measured on crystals at 130 K. Structures were determined using direct methods and refined using a full-matrix

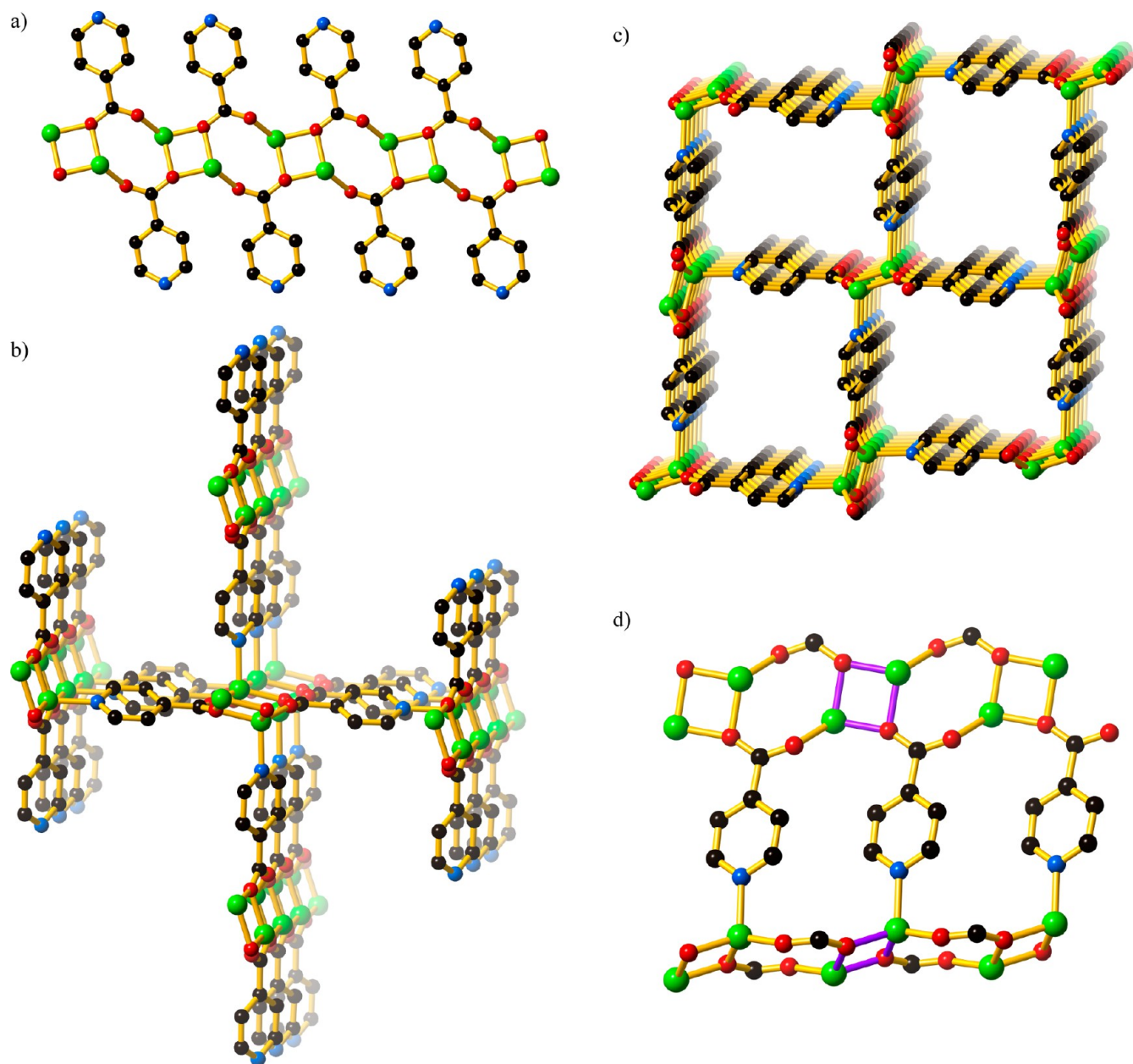


Figure 1. Structure of Li(inic)·0.5morpholine. (a) A Li(inic) 8484 chain or strip in Li(inic)·0.5morpholine. (b) A central strip seen here almost end-on, connected to four other strips by N–Li bonds. The upper and lower strips provide the N centers for the N–Li bonds to the central strip. The N centers for the N–Li bonds to the left and right strips are provided by the central strip. (c) The extended 3D network. (d) The *cis* disposition of 4-membered rings in Li(inic)·0.5morpholine (highlighted in purple).

least-squares procedure based on F^2 .^{16,17} Crystal data and refinement details are presented in Table 1. Detailed information regarding the refinement of each of the structures is included in the Supporting Information.

Powder diffraction patterns were recorded on an Oxford Diffraction Supernova diffractometer using Cu $K\alpha$ radiation or on the powder diffraction beamline at the Australian Synchrotron using radiation of wavelength 0.7796 or 0.7907 Å.

Thermogravimetric Analyses. Thermogravimetric analyses were performed on an SDDTA851 Mettler-Toledo analyzer; analyses were performed on freshly prepared samples under a nitrogen atmosphere.

Gas Sorption Measurements. Gas sorption data were measured using a Sieverts-type BELsorp-HP automatic gas sorption apparatus (BEL Japan Inc.). Ultrahigh purity gases were used for sorption studies.

RESULTS

In the preliminary communication, three solvates of composition Li(inic)·*S*, in which *S* = 0.5 morpholine, 0.5 *N*-methylpyrrolidinone, and 0.5 *N,N*-dimethylformamide, were reported as sharing a common 3D framework structure in which 4-coordinate Li⁺ ions are bridged by an isonicotinate anion that binds to four Li⁺ centers.¹⁵ More recently we have discovered that not only does the morpholine solvate differ structurally and topologically from the other two, but that other solvated forms of Li(inic) can be obtained, exhibiting what may be described as framework isomerism. Numerous Li(inic) polymeric structures have now been identified. The generation of many of these new compounds relies mainly, although not exclusively, upon a synthetic approach described in the earlier

work that allows crystallization from a solvent in which the components (Li^+ and inic^-) exhibit very low solubility.¹⁵

Seven different types of structures have been identified which for convenience have been classified as types **Ia**, **Ib**, **Ic**, **II**, **III**, **IV**, and **V** according to the topology of the network. The type **Ia**, **Ib**, and **Ic** compounds share a similar 3D network structure with subtle but nevertheless significant topological differences between them. Types **II**, **III**, and **IV** are also 3D network structures that exhibit pronounced differences between each other and the type **I** structures. The type **V** structure is a hydrate and has a densely packed chain structure. Remarkable crystal transformations including a number of single-crystal-to-single-crystal transformations between different structural types can be achieved through solvation and desolvation processes.

Crystals, suitable for X-ray diffraction studies, of composition $\text{Li}(\text{inic})\cdot\text{S}$ ($\text{S} = 0.5$ morpholine (**Ia**), 0.5 dioxane (**Ia**), 0.25 *n*-hexanol (**Ia**), 0.5 *N*-methylpyrrolidinone (**Ib**), 0.5 *N,N*-dimethylformamide (**Ib**), 0.5 *n*-propanol (**Ib**), 0.5 pyridine (**Ib**), 0.5 cyclohexanol (**Ib**), 0.5 *t*-butanol (**Ic**), 0.5 methanol (**II**), and 0.5 ethanol (**II**), are obtained by reaction of LiOH with isonicotinic acid in the appropriate solvent (or mixture of solvents).

Type Ia Li(inic) Networks: $\text{Li}(\text{inic})\cdot\text{S}$, $\text{S} = 0.5$ Morpholine, 0.5 Dioxane, 0.25 *n*-Hexanol. Strip-like $\text{Li}(\text{inic})$ chains consisting of alternating 8-membered $\text{Li}-\text{O}-\text{C}-\text{O}-\text{Li}-\text{O}-\text{C}-\text{O}$ rings and 4-membered $\text{Li}-\text{O}-\text{Li}-\text{O}$ rings fused together as in Figure 1a can be discerned in the structure of the morpholine solvate. We refer to such chains, which are also seen in the other type **I** structures, as 8484 chains. All the 8484 chains in the morpholine solvate are equivalent and parallel although the average planes of half of them are oriented differently from those of the other half. Any strip is connected to four others by $\text{N}-\text{Li}$ bonds as indicated in Figure 1b. The upper and lower strips in Figure 1b provide the nitrogen centers for the $\text{N}-\text{Li}$ bonds to the central strip, which in turn provides the nitrogen centers for the $\text{N}-\text{Li}$ bonds to the left and right strips. As can be seen in Figure 1b the average plane of the central 8484 strip is close to perpendicular to the planes of the other four attached strips. In this way the Li^+ cations acquire a roughly tetrahedral environment consisting of three carboxylic oxygen centers and one nitrogen center, and the extended 3D structure containing solvent-filled channels, as shown in Figure 1c, is generated. The morpholine molecules located in the channels are very disordered, but our modeling of the disorder suggests that the morpholine NH group, surprisingly, is not within hydrogen-bonding range of any of the inic^- oxygen atoms. The structure of $\text{Li}(\text{inic})\cdot 0.5\text{dioxane}$ is very similar to the morpholine solvate (see Supporting Information) with dioxane molecules located in the approximately square channels; half of the guest dioxane molecules are disordered. $\text{Li}(\text{inic})\cdot 0.25n\text{-hexanol}$ also has a type **Ia** structure. While the guest molecules are disordered it was possible to model the *n*-hexanol over two sites. One orientation of the *n*-hexanol within the channel is shown in Figure 2; the hexanol oxygen atom is located 3.01 Å from the nearest inic^- oxygen atom. Whereas $\text{Li}(\text{inic})\cdot 0.25n\text{-hexanol}$ has the same topology as the morpholine and dioxane solvates, there are structural differences relating to an alternation in the orientation of the pyridyl groups along the length of the channel walls which are linked to the location and conformation of the relatively long *n*-hexanol molecule. This leads to an approximate doubling of the *a* axis and the adoption of a monoclinic rather than a triclinic space group.

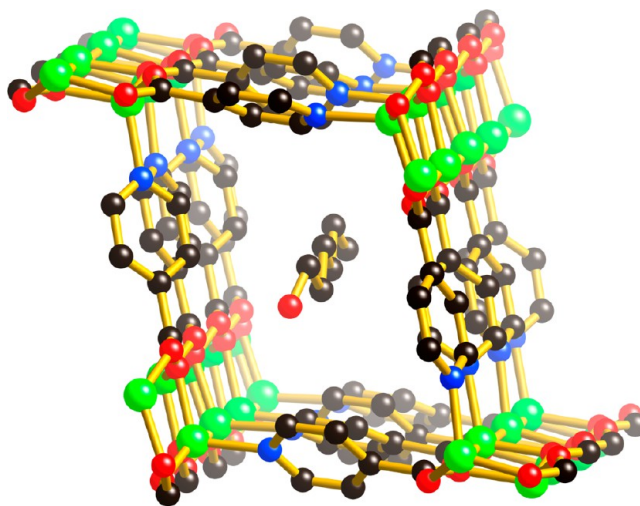


Figure 2. One orientation of the disordered *n*-hexanol molecule in $\text{Li}(\text{inic})\cdot 0.25n\text{-hexanol}$.

A feature of the **Ia** structure that distinguishes it from the type **Ib** and **Ic** structures described below relates to the geometrical disposition of the two 4-membered $\text{Li}-\text{O}-\text{Li}-\text{O}$ rings directly associated with any inic^- anion. At the carboxy end of the inic^- anion, one of the carboxy oxygen atoms forms part of a 4-membered ring, and at the other end the nitrogen atom associates directly with a lithium ion that forms part of another 4-membered ring. In the **Ia** structure, these two 4-membered rings, directly associated with any particular inic^- anion, are disposed *cis* to each other, as is shown in Figure 1d. In contrast, the two 4-membered rings associated with any inic^- unit in some of the derivatives described below are disposed in a *trans* manner, while in yet another case both *cis* and *trans* dispositions are seen in the same structure.

Type Ib Li(inic) Networks: $\text{Li}(\text{inic})\cdot\text{S}$, $\text{S} = 0.5$ *N*-Methylpyrrolidinone, 0.5 Dimethylformamide, 0.5 *n*-Propanol, 0.5 Cyclohexanol, 0.5 Pyridine. These five compounds have a common $\text{Li}(\text{inic})$ framework structure, which resembles that just described for the **Ia** structures and contains 8484 strips almost identical to that shown in Figure 1a, but now the two 4-membered rings associated directly with any inic^- anion are disposed in a *trans* fashion, as shown in Figure 3a (which pertains specifically to the *N*-methylpyrrolidinone compound, but the other four are essentially identical). The essential topological difference between type **Ia** and type **Ib** networks can be appreciated upon comparison of Figures 3a and 1d. The *N*-methylpyrrolidinone guests located in the channels are well-ordered. Figure 3b shows a channel containing *N*-methylpyrrolidinone guests. The oxygen atom of *N*-methylpyrrolidinone makes a contact of 3.37 Å to a pyridine β carbon atom of the framework. The structure of $\text{Li}(\text{inic})\cdot 0.5\text{DMF}$ is closely similar to that just described for $\text{Li}(\text{inic})\cdot 0.5N\text{-methylpyrrolidinone}$, but with the guest molecules exhibiting some degree of disorder. Figure 3c shows one orientation of a dimethylformamide guest within a “belt” of four inic^- units that comprise the nearest components of the channel walls.

The pyridine and cyclohexanol solvates adopt a very similar structure to the *N*-methylpyrrolidinone and *N,N*-dimethylformamide solvates described above. The guest pyridine molecules are located in the channels and lie in an orientation parallel to the plane of half of the coordinated pyridyl groups. Alternation

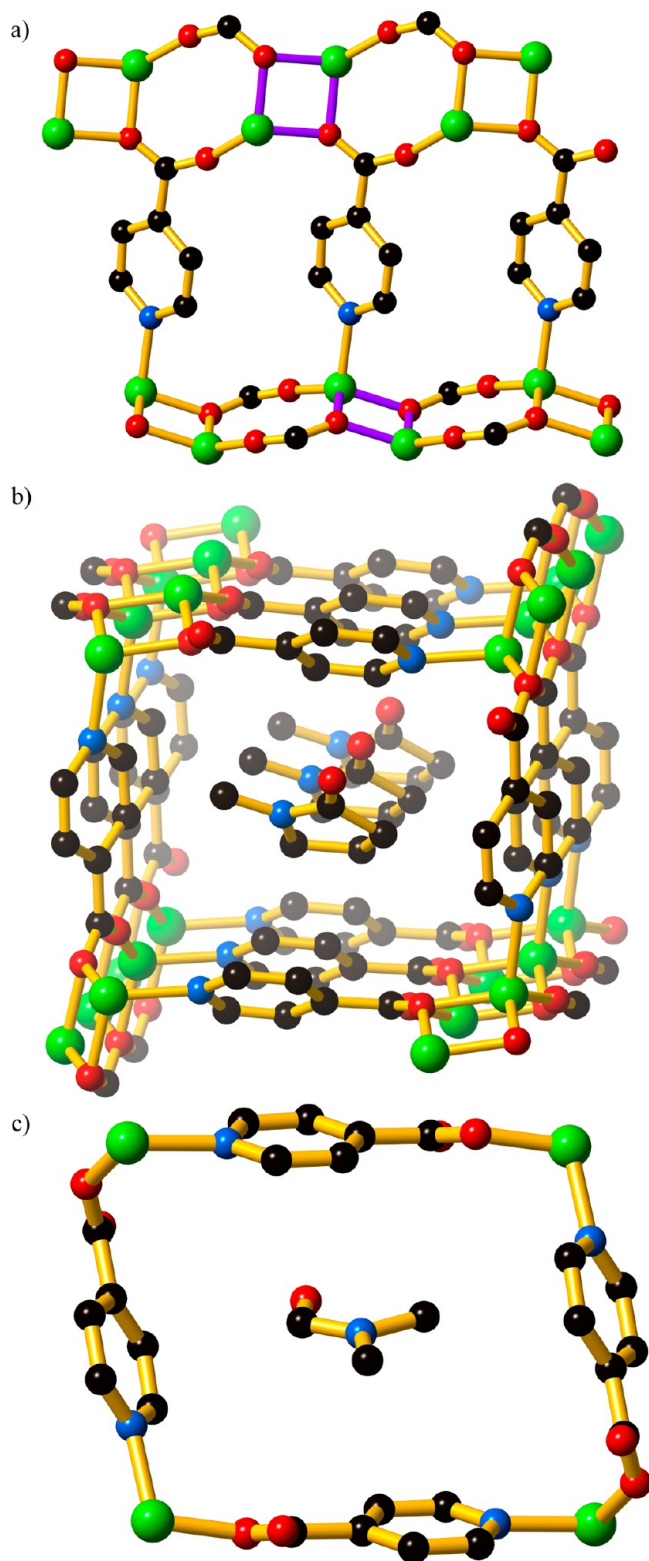


Figure 3. (a) The *trans* disposition of 4-membered rings in $\text{Li}(\text{inic}) \cdot 0.5N\text{-methylpyrrolidinone}$ (highlighted in purple). (b) One orientation of the *N*-methylpyrrolidinone guest in the channel. (c) One orientation of the *N,N*-dimethylformamide guest in a channel in $\text{Li}(\text{inic}) \cdot 0.5\text{dimethylformamide}$; only the four near-neighbor inic^- units are shown here.

in the orientation of the pyridine molecules occurs from one channel to the next, as is indicated in Supporting Information.

Some disorder associated with the location of the nitrogen atom within the aromatic ring is present with the pyridine located on a center of inversion. The cyclohexanol solvate contains channels filled with cyclohexanol molecules, which are also disordered across a center of inversion. One minor difference between this structure and the three previously described structures is that the inic^- bridging anions appear somewhat bowed, presumably a consequence of the channels expanding to accommodate the bulky cyclohexanol molecules (see Supporting Information).

In $\text{Li}(\text{inic}) \cdot 0.5n\text{-propanol}$ the $\text{Li}(\text{inic})$ framework has the same topology as the aforementioned type **Ib** structures, but now there are two different types of *n*-propanol guests in equal proportions, both well-defined in the structure. As can be seen in Figure 4, one *n*-propanol guest is hydrogen-bonded to an

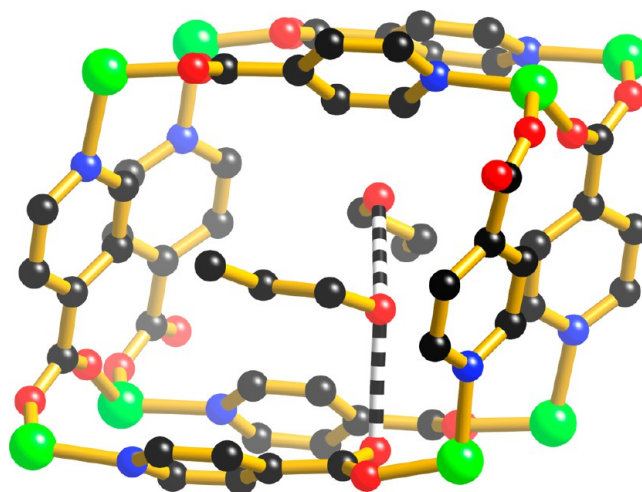


Figure 4. The two different types of *n*-propanol in $\text{Li}(\text{inic}) \cdot 0.5n\text{-propanol}$. Hydrogen bonds are represented by banded connections. The four pyridine units surrounding the *n*-propanol molecule hydrogen-bonded to inic^- (ie the one nearer the viewer) are intrinsically different from the four surrounding the other type of *n*-propanol.

inic^- oxygen atom ($\text{O}-\text{H} \cdots \text{O}$, 2.89 Å), and the other is hydrogen-bonded to the first ($\text{O}-\text{H} \cdots \text{O}$, 2.82 Å). As is also apparent in Figure 4, the belts of four pyridine units surrounding the two different sorts of propanol are themselves different. As a result of the presence of the two different types of propanol unit extending along the channel, the cell dimension in the channel direction (parallel with the *a* axis) is doubled (10.8093(1) Å) compared with those in the other solvated compounds (5.3881(8) to 5.4733(1) and 5.4028(1) Å).

Type Ic Li(inic) network: $\text{Li}(\text{inic}) \cdot 0.5t\text{-butanol}$. The *t*-butanol-solvated compound possesses a $\text{Li}(\text{inic})$ framework structure that differs yet again from those seen in either the type **Ia** frameworks with *cis* 4-membered rings or the type **Ib** frameworks with *trans* 4-membered rings. In the *t*-butanol-solvated network half the inic^- units have a *trans* arrangement of the directly associated 4-membered rings and the other half have a *cis* arrangement, as is shown in Figure 5a. Two adjacent walls of a channel are shown in Figure 5a, inspection of which will reveal that the upper group of three inic^- units are associated with a *trans* arrangement of 4-membered rings, while the lower inic^- units are associated with *cis*-disposed 4-membered rings. The channels, which are shown in Figure 5b,

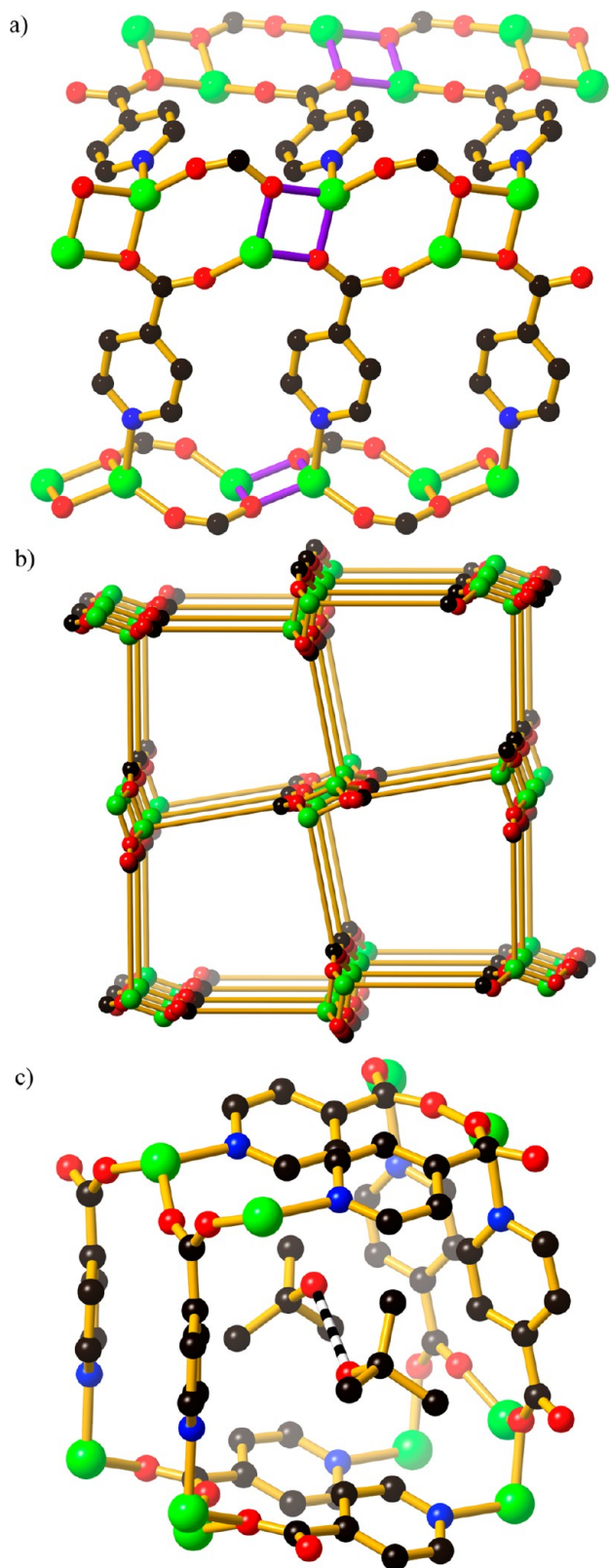


Figure 5. (a) Two adjacent channel walls in $\text{Li}(\text{inic})\cdot 0.5t\text{-butanol}$, the upper wall having inic^- units with a *trans* disposition of 4-rings and the lower one having *cis* arrangements (represented in purple). (b) The distorted channels in $\text{Li}(\text{inic})\cdot 0.5t\text{-butanol}$. Each pyridine unit here has been replaced by a rod directly connecting the carboxylate carbon atom to lithium. (c) A hydrogen-bonded pair of *t*-butanol guests surrounded by two belts, each containing four inic^- units.

are now considerably distorted from the parallelogram-like cross-section seen in the “all-*trans*” and “all-*cis*” compounds. The *t*-butanol guests appear in hydrogen-bonded pairs ($\text{O}\cdots\text{O}$, 2.85 Å) and are each disordered over two sites: one arrangement is shown in Figure 5c.

Type II Li(inic) Networks: $\text{Li}(\text{inic})\cdot 0.5 \text{ MeOH}$ or 0.5 EtOH . The structures of $\text{Li}(\text{inic})\cdot 0.5 \text{ ROH}$ ($\text{R} = \text{Me}$ or Et) differ significantly from those considered above. We describe the methanolate here. Chains of the 8484 type, much the same as those seen in all the above cases (such as that in Figure 1a), are also present in the methanolate. Now, however, as can be seen in Figure 6a, each of the two lithium centers in one 8-membered ring is attached to a molecule of methanol, the two being oriented *trans* to each other, while the Li centers in the next 8-membered ring are associated with two pyridine nitrogen centers, again in a *trans* relationship. All the chains are equivalent and parallel. Two sorts of isonicotinate unit are present in equal numbers; one type associates via its N atom with a Li^+ cation in another chain, and the second type is H-bonded via its N atom to a methanol molecule associated with yet another chain (see Figure 6a). The extended 3D network is shown in Figure 6b in which the 8484 chains are seen almost end-on. For simplicity and clarity the isonicotinate units directly linked via nitrogen to lithium are represented in Figure 6b by amber rods connecting the carboxylate carbon atom to the lithium center, and the inic^- units involved in H-bonding are represented as magenta rods. An interesting feature of the methanolate structure, of relevance to mechanistic considerations presented below, is that those inic^- units that are N-bonded to Li centers are associated with a *cis* disposition of 4-membered rings as shown in Figure 6c.

Type III Li(inic) Network: Solvent-Free Li(inic). The removal of solvent from the variously solvated $\text{Li}(\text{inic})$ derivatives, simply by heating, promotes the remarkable framework rearrangement described in detail below, generating the same solvent-free $\text{Li}(\text{inic})$ in all cases. We were able to observe single-crystal-to-single-crystal transformations and carry out single-crystal X-ray diffraction structural studies on the desolvated products in the cases of the *n*-hexanol-solvated crystals (type Ia, in which the 4-membered rings are disposed *cis*), *N,N*-dimethylformamide-solvated crystals (type Ib, with a *trans* disposition of 4-membered rings), and the methanol-solvated crystals (type II). X-ray powder diffraction studies of the desolvated products from the morpholine-, *n*-propanol-, and *t*-butanol-solvated derivatives indicate that the same $\text{Li}(\text{inic})$ structure is generated in these cases also. The thermogravimetric traces for the solvated compounds, which are presented in Figure 7 (for the *n*-hexanol solvate) and in Supporting Information (for the remaining compounds), indicate that the solvent-free $\text{Li}(\text{inic})$ shows high thermal stability, with no significant weight loss being observed after solvent removal up to temperatures in excess of 350 °C.

The structure of desolvated $\text{Li}(\text{inic})$ contains chains, shown in Figure 8a, consisting of fused 6-membered rings, hereafter referred to as 6666 chains; these are to be contrasted with the 8484 chains present in the solvated precursor. Individual $\text{Li}(\text{inic})$ 6666 chains are chiral, as can be appreciated upon examination of Figure 8a, with the two enantiomers occurring in equal numbers. All chains are parallel, and all inic^- units are equivalent. The extended 3D structure is shown in Figure 8b in which the 6666 chains are seen almost end-on. For clarity, the inic^- units are represented by rods connecting the carboxylate carbon atom to the lithium center. Channels running parallel

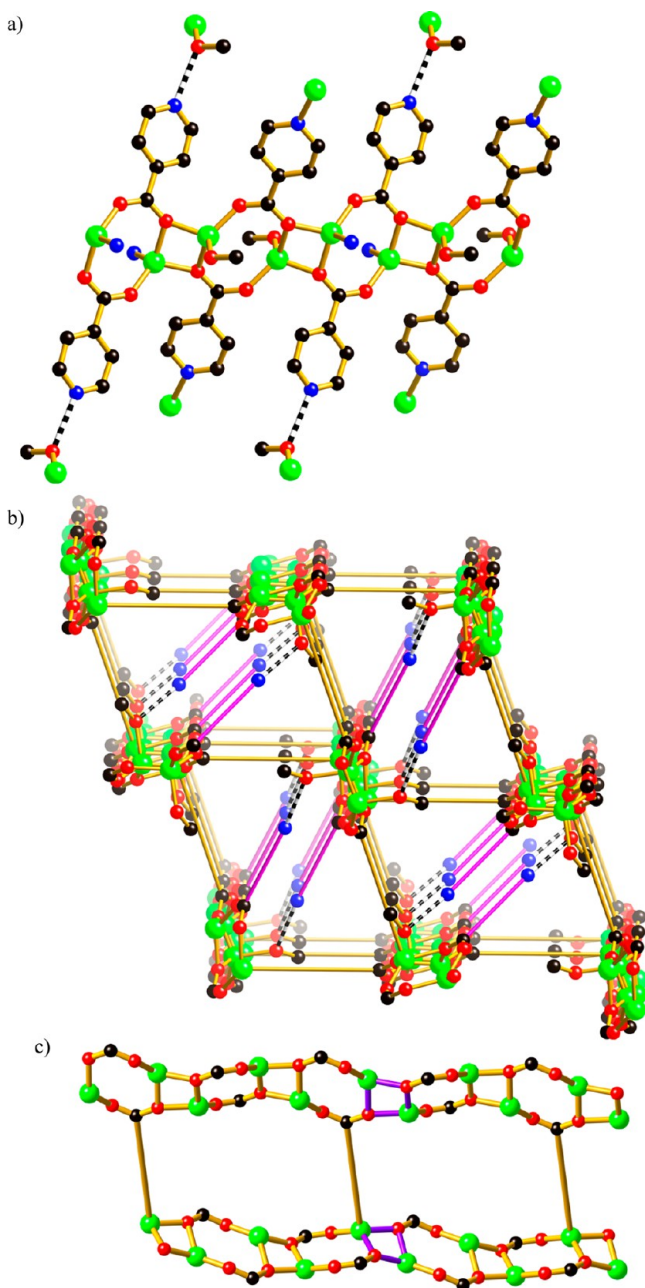


Figure 6. (a) Part of the 8484 carboxylate/Li⁺ chain and the appended pyridine and methanol units present in Li(inic)·0.5MeOH. One type of inic⁻ unit associates via its nitrogen center with a Li⁺ cation in another chain. The second type of inic⁻ unit is hydrogen-bonded to a methanol molecule attached to a different chain. There are two sorts of 8-membered rings; one sort carries two *trans* MeOH molecules and the other two *trans* pyridine units, only the N atoms of which are shown here. (b) The extended 3D structure of Li(inic)·0.5MeOH. The 8484 chains are seen here almost end-on. The magenta rods represent the inic⁻ units whose N centers are hydrogen-bonded to methanol. The amber rods represent the inic⁻ units whose N centers make bonds to Li; in this case the rods connect the carboxylate carbon atom directly to the Li center. (c) The *cis* disposition of 4-membered rings around those inic⁻ units N-bonded to Li in Li(inic)·0.5MeOH. The inic⁻ units making N–Li bonds are represented here by amber rods that connect the carboxylate carbon atom directly to the Li center.

with the chains can be seen. The individual channels themselves have a helical character, half of them resembling a right-handed

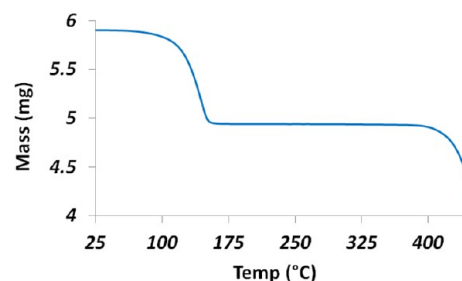


Figure 7. TGA of Li(inic)·0.25*n*-hexanol.

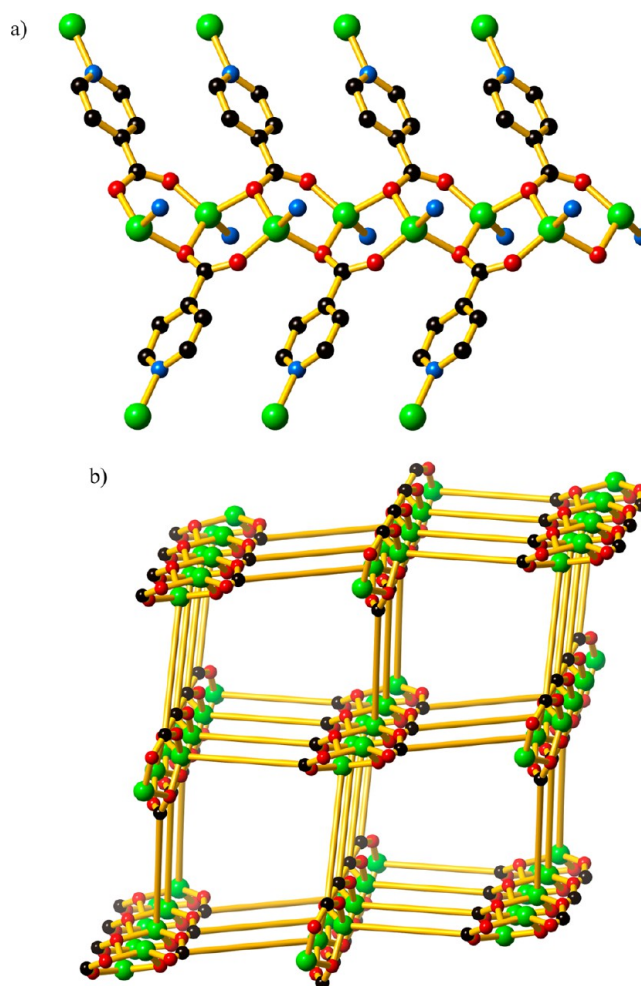


Figure 8. (a) Part of the 6666 Li(inic) chain in solvent-free Li(inic). Each individual chain is chiral. Attached to the lithium centers above and below the chain are pyridine components of other chains, only the N atoms of which are shown. (b) The extended 3D structure of Li(inic). For clarity, the isonicotinate units are represented by rods connecting the carboxylate carbon atom to the lithium center. Each chain is linked to four other parallel chains of the other absolute configuration. The central chain and the four chains at the corners have the same absolute configuration and are related by simple translations. The other four chains have the other absolute configuration and are likewise related by translations.

screw, and the others being left-handed. In Figure 8b the central chain and the ones seen at the four corners, being all of the same hand, are related by simple translations; the other four chains visible in the figure, all of the other hand, also are interrelated by simple translations. A characteristic feature of the structure of desolvated Li(inic) is the herringbone-like

disposition of the inic^- units projecting from the Li/O/C spine, which can be clearly seen in Figure 8a, and which is to be contrasted with the parallel disposition of the projecting inic^- units seen in the other structures described above; this parallel disposition is, for example, apparent in Figure 1a. This herringbone-like structural feature of solvent-free $\text{Li}(\text{inic})$ is pursued further in mechanistic considerations presented in the Discussion section.

A significant difference between the type I and type III structure relates to the size of the framework channels. Taking $\text{Li}(\text{inic})\cdot 0.5N$ -methylpyrrolidinone as a typical example, the van der Waals intraframework space represents 31% of the crystal volume.¹⁸ Following desolvation and rearrangement to the type III structure, the intraframework space (which is now unoccupied) is only 19%. A comparison of the channel sizes in the two structures, presented in Figure 9, clearly shows that the channels are much narrower in the type III structure.

The generation of the type III structure upon desolvation prompted an investigation of the reversibility of this process. When crystals possessing the type III structure are immersed in DMF, a resolution process occurs leading to the generation of $\text{Li}(\text{inic})\cdot 0.5\text{DMF}$ (type Ib). Although the single-crystal character is lost in the process, the formation of $\text{Li}(\text{inic})\cdot 0.5\text{DMF}$ (type Ib) is indicated by powder diffraction. When type III crystals are immersed in carbon disulfide a remarkable single-crystal-to-single-crystal transformation occurs to generate the previously unknown solvate, $\text{Li}(\text{inic})\cdot 0.25\text{CS}_2$. Following immersion in carbon disulfide the crystal undergoes significant deterioration with single-crystal diffraction studies showing arch-shaped reflections indicating that the crystalline sample lies somewhere between a single crystal and a powder. Although the $\text{Li}(\text{inic})\cdot 0.25\text{CS}_2$ crystal obtained following immersion in carbon disulfide is of a poor quality, the structure determination and refinement clearly indicates the atom to atom connectivity of the $\text{Li}(\text{inic})$ network which has a type Ib structure. The linear CS_2 molecule is disordered over a pair of equivalent sites with 50% occupancy in each site. The CS_2 molecule, which is inclined to the channel direction, is located on a center of inversion, and makes contact with the carboxylate carbon atoms at each end, with a S...C separation of 3.5 Å (see Supporting Information Figure S4).

Type IV $\text{Li}(\text{inic})$ (Nonsolvated). Attempts to include *t*-amyl alcohol in the channels of a $\text{Li}(\text{inic})$ framework using the approach successfully employed for the solvated crystals described above proved unsuccessful; however, somewhat surprisingly, a nonsolvated form of $\text{Li}(\text{inic})$ was obtained which is distinctly different from the type III structure. Crystals of $\text{Li}(\text{inic})$ possess a dense 3D structure which contains parallel Li–carboxylate chains linked to equivalent chains through pyridyl bridges. The chains represented in Figure 10a may be considered as “double-decker” chains with symmetry-related lower and upper halves each resembling the 6666 chains that are a feature of the type III structure. In this dense structure there are two different inic^- ligands, one of which has a μ_3^- coordination mode, similar to that found in the type III structures, while the second has a μ_4^- coordination mode. The μ_4^- carboxylate is responsible for linking the two 6666 chains thereby generating the double-decker chain.

Inspection of Figure 10a reveals that half the Li^+ centers are in a tetrahedral environment formed by four oxygen atoms from within the chain; the remaining Li^+ centers are each bound to only three oxygen atoms. A tetrahedral coordination environment for this second type of Li^+ center is completed by

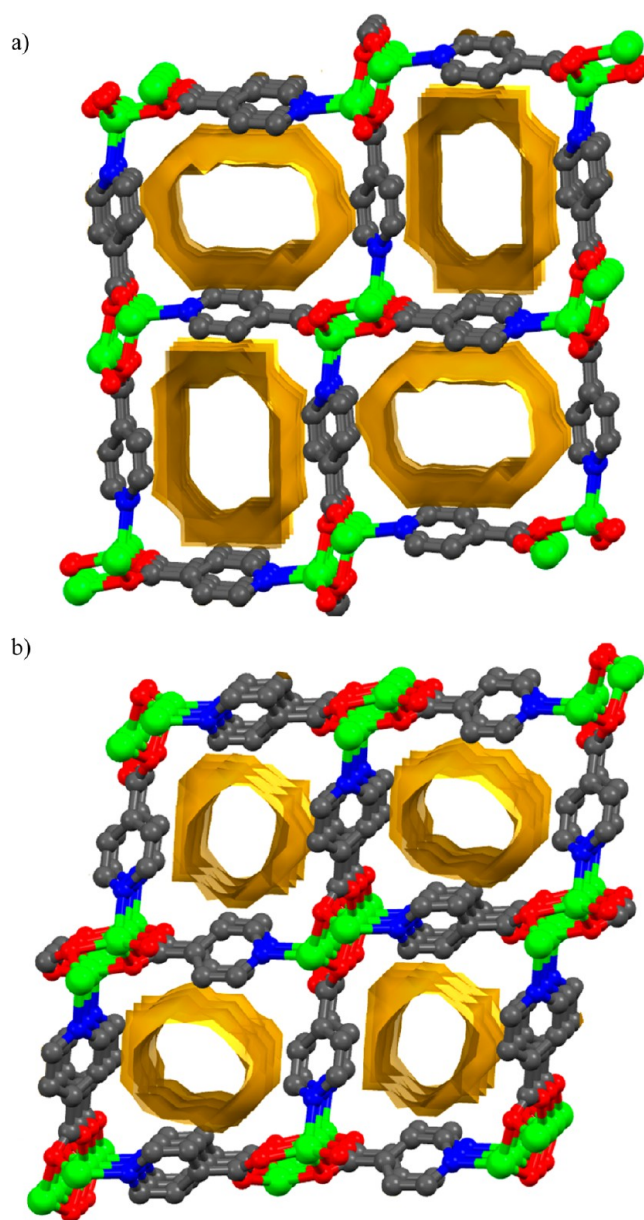


Figure 9. Representations of the van der Waals channel surfaces (yellow) in a) $\text{Li}(\text{inic})\cdot 0.5N$ -methylpyrrolidinone and b) $\text{Li}(\text{inic})$, type III. Although not shown, the van der Waals surfaces include the contribution of the hydrogen atoms that are part of the inic^- anion.

a nitrogen atom of an inic^- anion from a neighboring chain. Each double-decker chain acts as a pyridyl group acceptor from a pair of parallel chains that have a different orientation and are located on opposite sides of the chain (Figure 10b). As is also apparent in Figure 10b, pyridyl groups extend outward in opposite directions from the double-decker chains and form bridges to neighboring chains where they act as donors toward Li^+ centers within double-decker chains, again with a different orientation. It is noted that only half the inic^- anions form links between chains; the pyridyl groups of inic^- anions with the μ_4^- carboxylate coordination mode have uncoordinated pyridyl groups.

Type V $\text{Li}(\text{inic})\cdot 2\text{H}_2\text{O}$. The final type of structure found for the $\text{Li}(\text{inic})$ series is the hydrate which fails to form a 3D network through direct Li– inic connections. As indicated in Figure 11a the structure consists of chains of Li^+ centers

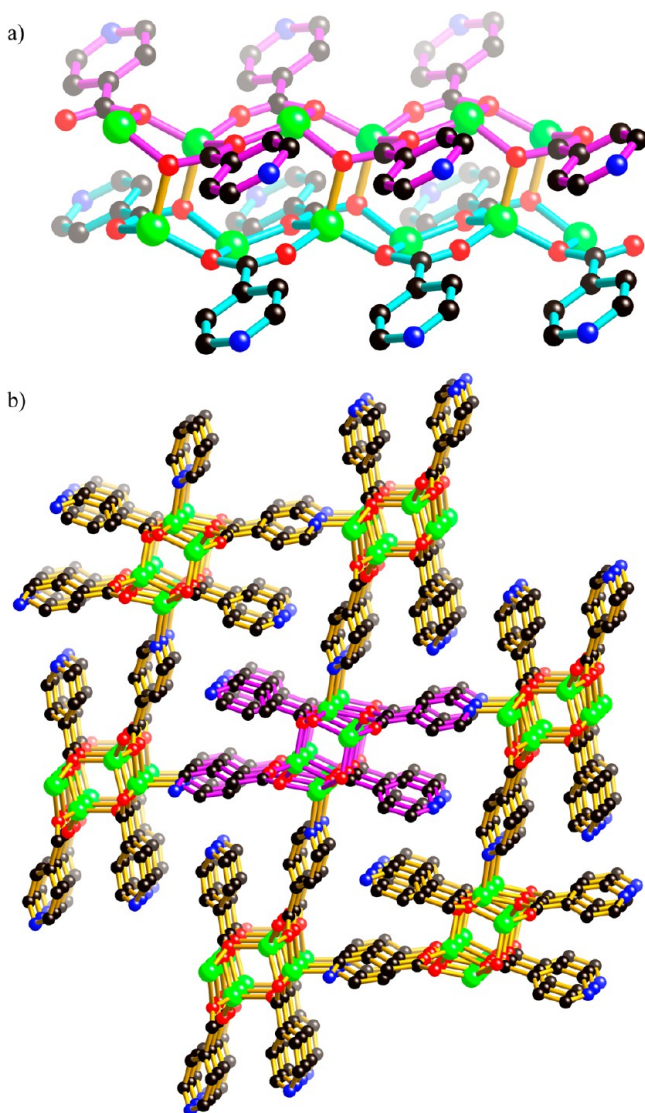


Figure 10. Structure of Li(inic) (type IV) showing (a) a “double-decker” Li(inic) chain and (b) the extended 3D network.

bridged by carboxylate groups and water molecules. The pyridyl groups do not coordinate to Li^+ centers but rather participate in hydrogen-bonding interactions with the bridging water molecules. As a result a 3D hydrogen-bonded network is obtained in which parallel lithium–water–carboxylate chains are linked through pyridyl bridges to equivalent parallel chains as shown in Figure 11b.

Interestingly the exposure of the type IV structure to the atmosphere over a period of a day results in the conversion to the type V hydrate structure. As indicated by powder diffraction studies (see Supporting Information), this process is reversible with conversion back to the type IV structure upon heating. Formation of the hydrate structure also occurs when type I crystals are exposed to the atmosphere for extended periods; this process, however, is irreversible.

Gas Sorption Studies. In the original report describing *N,N*-dimethylformamide, morpholine, and *N*-methylpyrrolidone solvates, the gas sorption measurement were also reported. In the original investigation the sample used was obtained by desolvation of $\text{Li(inic)} \cdot 0.5\text{DMF}$. In order to make an accurate assessment of the sorption capacity it is necessary

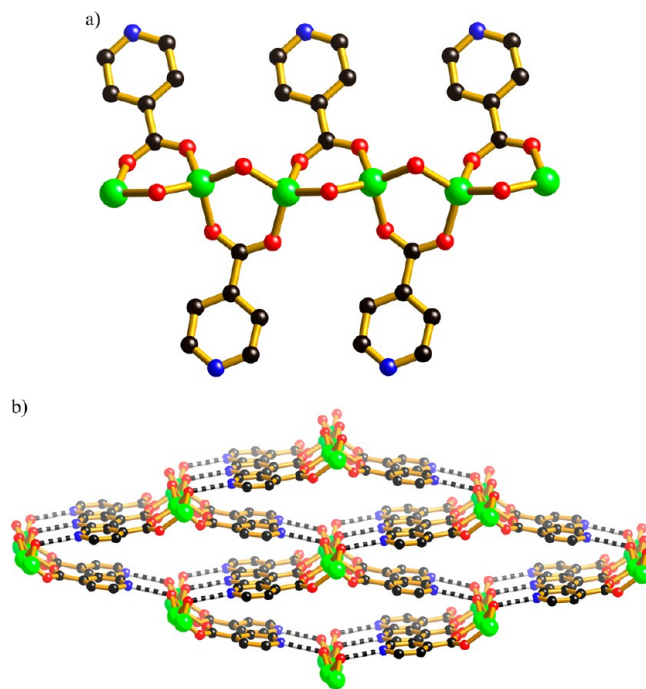


Figure 11. (a) Structure of Li(inic)·2H₂O (type V) showing (a) a single chain in Li(inic)·2H₂O in which lithium centers are bridged by carboxylate groups and water molecules and (b) the 3D network of Li(inic)·2H₂O with hydrogen bonds represented by striped connections.

to ensure that intraframework spaces are completely empty at the commencement of the isotherm measurement. The desolvation process is likely to be more successful when the guest molecules are volatile. We now present the 77 K H₂ isotherm obtained on a sample of $\text{Li(inic)} \cdot 0.5n\text{-propanol}$ which has undergone desolvation. While the shape of the isotherm (Figure 12) is similar to that originally reported, we note that the amount of H₂ sorbed is approximately 5% greater when the propanol solvate is used.

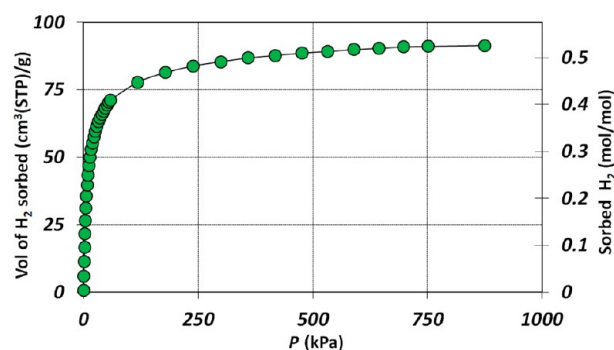


Figure 12. H₂ 77 K sorption isotherm for a baked sample of $\text{Li(inic)} \cdot 0.5n\text{-propanol}$.

DISCUSSION

Given the observed variety of framework structures described in the Results section, it does appear that the Li^+inic^- combination is unusually able to adapt to the size and shape demands of the templating guest. Although the structures of type Ia and Ib compounds are very similar, the surfaces of the channels in the two cases will no doubt be subtly different, with

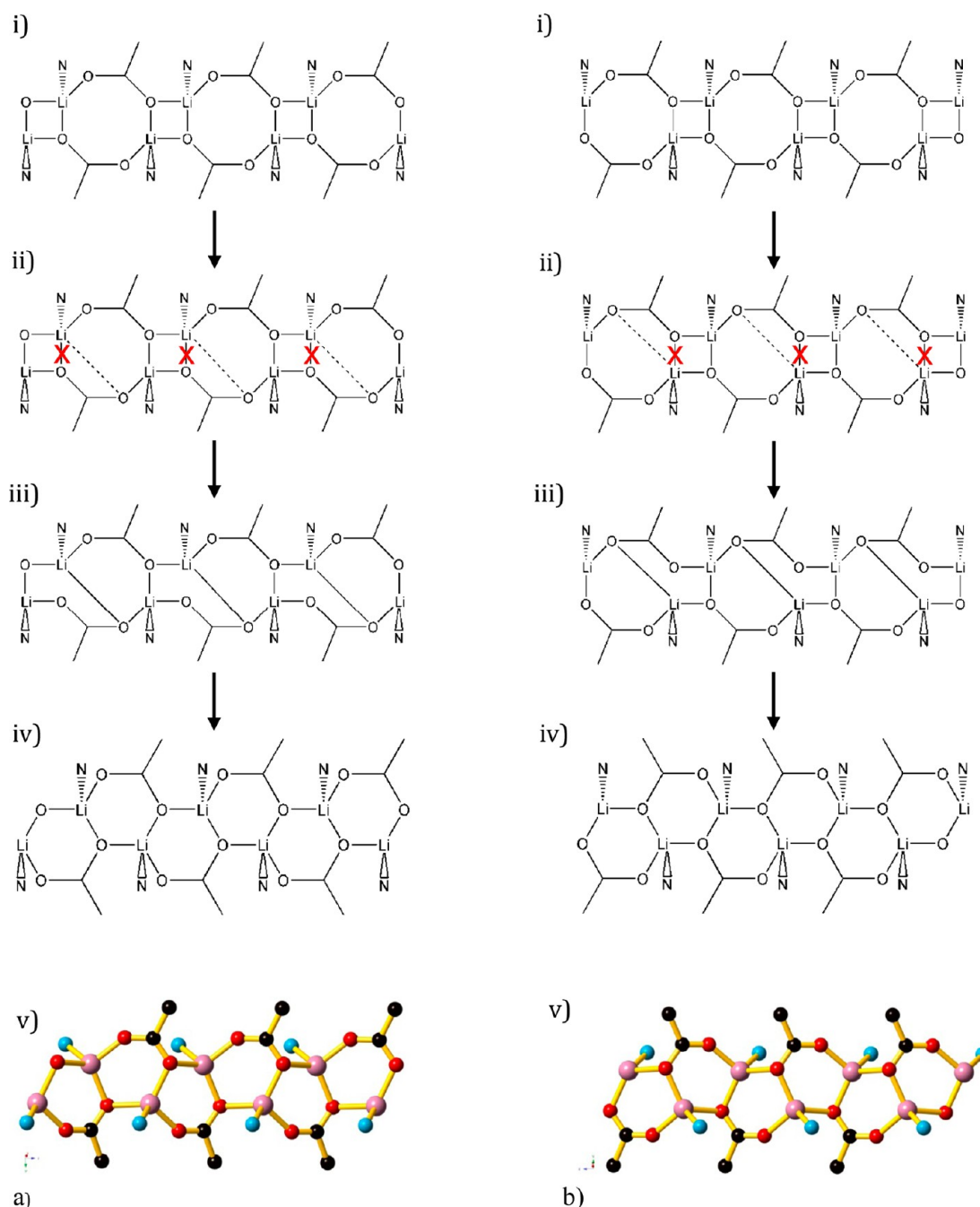


Figure 13. Proposed sequence of Li–O bond breaking and making involved in transforming the 8484 chains to chiral 6666 chains. Parts aii and bii indicate the Li–O bonds required to be broken and those to be made to generate the two enantiomeric 6666 chains seen in aiv and biv, respectively. Parts av and bv represent the real enantiomeric 6666 chains seen in the structure of solvent-free Li(inic), which can be seen to be identical to those shown in the schematic parts aiv and biv, respectively.

type **Ia** being compatible with the incorporation of disordered morpholine, dioxane, or *n*-hexanol and type **Ib** favoring the incorporation of disordered *N*-methylpyrrolidinone, *N,N*-dimethylformamide, *n*-propanol, cyclohexanol, pyridine, and carbon disulfide.

The type **Ic** framework, with half the inic units associated with a *cis* arrangement of the 4-membered rings and the other half associated with a *trans* arrangement and with the distinctly distorted channel seen in Figure 5b, is presumably able to maximize attractive nonbonded interactions between the pairs of guest *t*-butanol molecules and the surrounding channel surface.

In the alcohol-solvated series of compounds, interesting variations in the role played by the guest are observed. In the case of the bulky *t*-butanol the OH group fails to interact directly with the Li(inic) framework, whereas the less hindered hydroxyl group in the primary alcohols *n*-propanol and *n*-hexanol is able to form hydrogen bonds to an inic[−] oxygen center. The even less hindered methanol and ethanol are able to associate with the framework by forming direct Li⁺–O bonds.

We propose that the sequence of Li–O bond breaking and bond making processes represented in Figure 13 (links to an animated form are given in the Supporting Information)

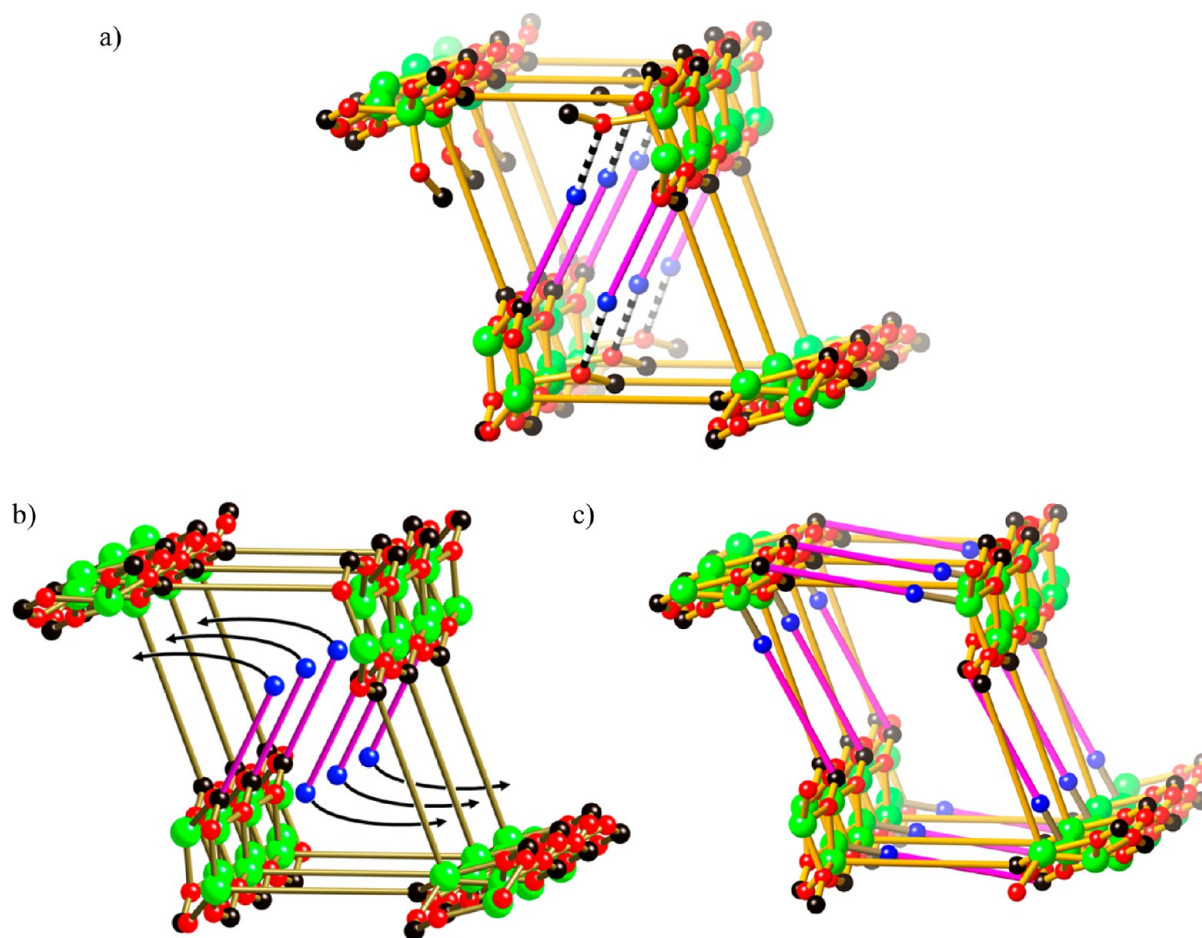


Figure 14. Proposed sequence of MeOH loss and swivelling of the pyridine units. (a) One “incipient channel” in $\text{Li}(\text{inic})\cdot 0.5\text{MeOH}$. The inic units hydrogen-bonded to methanol are here represented by magenta rods linking the nitrogen atom to the carboxylate carbon atom. (b) An incipient channel in $\text{Li}(\text{inic})\cdot 0.5\text{MeOH}$ with the MeOH removed, showing the directions in which the originally H-bonded inic units will pivot. The inic units already in the wall of the incipient channels are represented by amber rods connecting the carboxylate carbon atom to the Li center. (c) The channel structure after the initially H-bonded inic units have swung around to make new N–Li bonds. Very minor adjustments of bond distances and angles within the Li/carboxylate chains would be required to render equivalent the newly introduced wall components and the pre-existing ones.

accounts very satisfactorily for all the observed geometrical and topological aspects of the solid-state rearrangement process whereby 8484 chains are transformed into 6666 chains, generating microporous $\text{Li}(\text{inic})$. It is important to note that each carboxylate unit is associated with three lithium centers before and after the rearrangement. A central feature of our proposed mechanism is that any carboxylate unit remains associated with the same three lithium cations throughout the process. With regard to fluctuations in electrostatic energy during the process, this is an eminently reasonable assumption to make. This proposed sequence leads inevitably to 6666 chains that are chiral, a crucial fact about the structure of the real solvent-free $\text{Li}(\text{inic})$ (type III) for which our mechanism is required to account. In addition the proposed sequence leads inevitably to $\text{Li}(\text{inic})$ chains with the observed herringbone-like appearance. As can be seen in Figure 13, the absolute configuration of the chain formed is determined simply by which of the two Li–O bonds in the 4-membered ring is broken. Figures 13av and 13bv, which show the two enantiomeric 6666 chains observed in the real structure, are presented for comparison with those arising from the proposed sequence of steps; all the configurational details in the real, observed structure seen in Figures 13av and 13bv are faithfully

reproduced in the structures shown in Figures 13aiv and 13biv that the proposed sequence predicts.

We propose that the driving force for the rearrangement of the 8484 chains into 6666 chains arises in part from more favorable pyridine–pyridine interactions in the latter. The 6666 chains are considerably more convoluted than the 8484 chains and are thereby contracted along their length in concertina-fashion. A direct consequence of these contractions is that the distance from any atom within an inic[−] unit to the same atom in the nearest neighbor inic units is $\sim 10\%$ less for the 6666 structure [$4.920(2)$ Å] than for any of the 8484 structures (~ 5.4 Å). For the same reason, the volume per $\text{Li}(\text{inic})$ for solvent-free $\text{Li}(\text{inic})$ (~ 362 Å³) is of the order of 14% less than that for the 8484 structures (average ~ 415 Å³), consistent with tighter pyridine–pyridine interactions in the 6666 case.

In the particular case of the multistep generation of $\text{Li}(\text{inic})$ containing 6666 chains from $\text{Li}(\text{inic})\cdot 0.5\text{MeOH}$ with its type II structure, we propose that the first stage in the process is formation of a type I $\text{Li}(\text{inic})$ framework, as elaborated below and shown in Figure 14. In the structure of $\text{Li}(\text{inic})\cdot 0.5\text{MeOH}$ shown in Figure 14a, one can already see, in incipient form, the channels to be generated in the final product; they are occupied and blocked off at this stage by diagonally inclined H-bonded inic[−] units (the magenta rods in Figure 14a). The remainder of

the inic^- units (represented by amber rods in Figure 14a) form an already established part of what are to become the walls of the channel produced by the rearrangement. As referred to earlier and shown in Figure 6c, these inic^- units that already are N-bonded to Li are associated with a *cis* disposition of 4-membered rings. When the methanol molecules are lost from the structure, it is proposed that the isonicotinate units that had been H-bonded to methanol pivot around the O...O “hinge” of the carboxylate unit in the manner shown in Figure 14b; the N atoms of the pivoting inic^- units thereby move into positions close to those just vacated by methanol so as to come within bonding distance of the lithium cation. Figure 14 shows the three stages in the proposed process: the first stage (Figure 14a) with the H-bonded MeOH molecules still present, the second (Figure 14b) with the MeOH removed, and the third (Figure 14c) after the inic^- units have pivoted to establish the new N–Li interactions. Only minor readjustments within the Li/carboxylate chains would be thereafter required to render equivalent all inic^- units in the walls (the ones that were originally present as well as those that have pivoted), and the walls of the channel would now be complete and impenetrable, with pyridine units in shoulder to shoulder contact. The inic^- units that pivot to form new N–Li bonds inevitably become associated with a *cis* disposition of 4-membered rings, and the new network thus formed is of the type Ia. The origins of the completed left and right walls of the channel in Figure 14 are clearly apparent upon consideration of the proposed sequence of steps shown there. The inic^- components newly introduced into the upper and lower walls of the channel (shown as magenta rods) originate, in exactly the same way, from initially H-bonded isonicotinate units diagonally disposed in the incipient channels above and below that in Figure 14 (but for simplicity and clarity not shown there).

While there is certainly diversity in the structures reported here it is interesting to note some common features present in the type I–IV structures. In all of these structures Li^+ centers are bridged by carboxylate groups, leading to an infinite array of parallel chains. The arrangement of Li^+ ions and carboxylate groups within the chain leaves either half or all the Li^+ centers bound by only three oxygen atoms. At least half of the pyridyl groups associated with a single chain provide bridges to equivalent chains. Each chain serves as both a pyridyl donor and acceptor in forming links to four equivalent chains, resulting in a 3D network in which each chain is linked to four other chains. When pyridyl groups are uncoordinated they are located in spaces that would correspond to channels in structures where all pyridyl groups are coordinated to Li^+ centers. The hydrated structure (type V) also possesses parallel lithium–carboxylate chains, but the coordination of the water molecule blocks the opportunity for pyridyl groups to provide direct links between chains. Nevertheless, hydrogen-bonding interactions involving pyridyl groups and the coordinated water molecules again results in each chain linking to four equivalent chains within a 3D network.

This investigation provides an opportunity to comment upon the relative stability of the two nonsolvated forms of Li(inic), i.e., type III and type IV. Both forms may be obtained by removal of solvent from solvated forms of Li(inic), and both forms revert to the same hydrate upon exposure to moisture in the atmosphere. Importantly, however, only the type IV structure is produced when the hydrate is heated, suggesting that the type IV structure is thermodynamically more stable than type III. The question then arises as to why type III rather

than type IV structures result from the desolvation of the type I and type II structures. We believe that while some degree of structural rearrangement of the type I and II Li(inic) frameworks is able to occur upon loss of guest molecules, the type of major rearrangement that would be required to generate double-decker chains of the type IV structure is only possible via formation of the hydrated structure (type V). It appears that the presence of water facilitates the considerable reorganization of the network components required to generate the dense 3D type IV structure.

■ CONCLUDING REMARKS

The nondirectional character of the ionic forces between the lithium cation and the carboxylate anion referred to above, we suggest, bestows a degree of “plasticity” upon the Li^+inic^- chains that not only allows the systems to adopt the different framework arrangements described here, but also facilitates the remarkable 8484-to-6666 rearrangements. An important aspect of the mechanism proposed for the rearrangement is that the carboxylate anion is not required ever to part company with the three lithium cations with which it is initially associated. In the particular case of the demethanolation of $\text{Li}(\text{inic})\cdot 0.5\text{MeOH}$, it is proposed that the 8484-to-6666 rearrangement is preceded by the pivoting of inic^- units whose N centers had been initially hydrogen-bonded to coordinated methanol; in the proposed mechanism for this entire demethanolation/rearrangement process every inic^- anion remains associated with the same three Li^+ cations throughout. Although the amounts of N_2 , H_2 , CH_4 , and CO_2 sorbed by microporous solvent-free Li(inic) are not among the highest,¹⁹ the gas sorption results clearly indicate that simple salts of lightweight lithium together with appropriately chosen anions are able to provide microporous materials capable of reversibly sorbing considerable quantities of gases. The isonicotinate anion was chosen for the initial exploratory work described here, merely because it is one of the simplest monoanions imaginable that possesses an element of rigidity and that offers the possibility of associating with cations at both ends so as to generate channels. Many potentially fruitful variants on the isonicotinate building block that may afford microporous solids with bigger internal surface areas are readily envisaged. The prospect is therefore raised of a new class of essentially ionic but nevertheless microporous materials based on lightweight lithium (and elements nearby in the periodic table) possessing the sort of “plasticity” considered above, that arises from the nondirectional character of ionic interactions.

■ ASSOCIATED CONTENT

📄 Supporting Information

Single-crystal data in CIF format. Calculated and observed X-ray powder diffraction patterns. TGA traces and animations. Experimental information regarding the gas sorption studies. This material is available free of charge via the Internet at <http://pubs.acs.org>.

■ AUTHOR INFORMATION

Corresponding Authors

*Email: bfa@unimelb.edu.au. Fax: (+61) 3-9347-5180.

*E-mail: r.robson@unimelb.edu.au. Fax: (+61) 3-9347-5180.

Present Address

§ANSTO, New Illawara Road, Lucas Heights, NSW 2234, Australia.

Notes

The authors declare no competing financial interest.

ACKNOWLEDGMENTS

We gratefully acknowledge the financial support of the Australian Research Council. This work is supported by the Science and Industry Endowment Fund. Part of the research reported was undertaken at the powder diffraction beamline at the Australian Synchrotron, Victoria, Australia.

REFERENCES

- (1) *Handbook of Zeolites: Structure, Properties and Applications*; Wong, T. W., Ed.; Nova Publishers: Hauppauge, NY, 2009.
- (2) (a) Rawat, D. S.; Heroux, L.; Krunleviciute, V.; Migone, A. D. *Langmuir* **2006**, *22*, 234–238. (b) Migone, A. D.; Talapatra, S. *Encyclopedia of Nanoscience and Nanotechnology*, Vol. 4; Nalwa, H. S., Ed.; American Scientific Publishers: Los Angeles, 2004; 3, pp 749–767. (c) Rawat, D. S.; Furuhashi, T.; Migone, A. D. *Langmuir* **2008**, *25*, 973–976. (d) Callejas, M. A.; Ansón, A.; Benito, A. M.; Maser, W.; Fierro, J. L. G.; Sanjuán, M. L.; Martínez, M. T. *Mater. Sci. Eng., B* **2004**, *108*, 120–123.
- (3) Panella, B.; Hirscher, M.; Roth, S. *Carbon* **2005**, *43*, 2209–2214.
- (4) Murray, L. J.; Dincă, M.; Long, J. R. *Chem. Soc. Rev.* **2009**, *38*, 1294–1314.
- (5) Kondo, M.; Yoshitomi, T.; Seki, K.; Matsuzaka, H.; Kitagawa, S. *Angew. Chem., Int. Ed. Engl.* **1997**, *36*, 1725–1727.
- (6) (a) Shimomura, S.; Bureekaew, S.; Kitagawa, S. *Struct. Bonding (Berlin)* **2009**, *132*, 51–86. (b) Férey, G. *Struct. Bonding (Berlin)* **2009**, *132*, 107–134.
- (7) Suh, M. P.; Park, H. J.; Prasad, K. T.; Lim, D.-W. *Chem. Rev.* **2012**, *112*, 782–835.
- (8) Bhatia, S. K.; Myers, A. L. *Langmuir* **2006**, *22*, 1688–1700.
- (9) (a) Batten, S.; Turner, D.; Neville, S. *Coordination Polymers: Design, Analysis and Applications*; Royal Society of Chemistry: Cambridge, U.K., 2009. (b) Kolotilov, K.; Pavlishchuk, V. *Theor. Exp. Chem.* **2009**, *45*, 75–97. (c) Lin, X.; Telepeni, I.; Blake, A.; Dailly, A.; Brown, C.; Simmonds, J.; Zoppi, M.; Walker, G.; Thomas, K.; Mays, T.; Hubberstey, P.; Champness, N.; Schroder, M. *J. Am. Chem. Soc.* **2009**, *131*, 2159–2171. (d) Yang, S.; Lin, X.; Blake, A.; Walker, G.; Hubberstey, P.; Champness, N.; Schroder, M. *Nat. Chem.* **2009**, *1*, 487–493. (e) Chun, H.; Jung, H.; Koo, G.; Jeong, H.; Kim, D.-K. *Inorg. Chem.* **2008**, *47*, 5355–5359. (f) Li, Y.; Xie, L.; Liu, Y.; Yang, R.; Li, X. *Inorg. Chem.* **2008**, *47*, 10372–10377. (g) Rowsell, J.; Yaghi, O. *Angew. Chem., Int. Ed.* **2005**, *44*, 4670–4679. (h) Kesanli, B.; Cui, Y.; Smith, M. R.; Bittner, E. W.; Bockrath, B. C.; Lin, W. *Angew. Chem., Int. Ed.* **2005**, *44*, 72–75.
- (10) (a) Dincă, M.; Long, J. R. *J. Am. Chem. Soc.* **2005**, *127*, 9376–9377. (b) Banerjee, D.; Borkowski, L. A.; Kim, S. J.; Parise, J. B. *Cryst. Growth Des.* **2009**, *9*, 4922–4926.
- (11) Banerjee, D.; Parise, J. B. *Cryst. Growth Des.* **2011**, *11*, 4704–4720.
- (12) Ong, T. T.; Kavuru, P.; Nguyen, T.; Cantwell, R.; Wojtas, Ł.; Zaworotko, M. J. *J. Am. Chem. Soc.* **2011**, *133*, 9224–9227.
- (13) Nouar, F.; Eckert, J.; Eubank, J. F.; Forster, P.; Eddaoudi, M. *J. Am. Chem. Soc.* **2009**, *131*, 2864–2870.
- (14) (a) Wu, T.; Zhang, J.; Zhou, C.; Wang, L.; Bu, X.; Feng, P. *J. Am. Chem. Soc.* **2009**, *131*, 6111–6113. (b) Zhao, X.; Wu, T.; Zheng, T.-S.; Wang, L.; Bu, X.; Feng, P. *Chem. Commun.* **2011**, *47*, 5536–5538. (c) Zhao, X.; Wu, T.; Bu, X.; Feng, P. *Dalton Trans.* **2011**, *40*, 8072–8074. (d) Zhao, X.; Wu, T.; Bu, X.; Feng, P. *Dalton Trans.* **2012**, *41*, 3902–3905.
- (15) Abrahams, B. F.; Grannas, M. J.; Hudson, T. A.; Robson, R. *Angew. Chem., Int. Ed.* **2010**, *122*, 1087–1087.
- (16) Sheldrick, G. M. *Acta Crystallogr.* **2008**, *A64*, 112–122.
- (17) Farrugia, L. J. *J. Appl. Crystallogr.* **1999**, *32*, 837–838.
- (18) Spek, A. L. *Acta Crystallogr.* **2009**, *D65*, 148–155.
- (19) The following references describe examples of porous coordination polymers that exhibit exceptional CO₂, H₂, and CH₄

sorption capacities: (a) Farha, O. K.; Yazaydin, A. Ö.; Eryazici, I.; Malliakas, C. D.; Hauser, B. G.; Kanatzidis, M. G.; Nguyen, S. T.; Snurr, R. Q.; Hupp, J. T. *Nat. Chem.* **2010**, *2*, 944–948. (b) Furukawa, H.; Ko, N.; G, Y. B.; Aratani, N.; Choi, S. B.; Choi, E.; Yazaydin, A. Ö.; Snurr, R. Q.; O’Keeffe, M.; Kim, J.; Yaghi, O. M. *Science* **2010**, *329*, 424–428. (c) Yan, Y.; Xiang, L.; Yang, S.; Blake, A. J.; Dailly, A.; Champness, N. R.; Hubberstey, P.; Schröder, M. *Chem. Commun.* **2009**, 1025–1027. (d) Xue, M.; Liu, Y.; Schaffino, R. M.; Xiang, S.; Zhao, X.; Zhu, G.-S.; Qiu, S.-L.; Chen, B. *Inorg. Chem.* **2009**, *48*, 4649–4651.